17th World Conference on Earthquake Engineering, 17WCEE
Sendai, Japan - September 13th to 18th 2020

Displacement-controlled Seismic Design Method of Reinforced Concrete Frame with Steel Damper Column

R. Mukoyama[(1)], K. Fujii[(2)], C. Irie[(3)], R. Tobari[(4)], M. Yoshinaga[(5)], K. Miyagawa[(6)]

[(1)] *Graduate Student, Chiba Institute of Technology, s1524317xa@s.chibakoudai.jp*
[(2)] *Professor, Dr. Eng., Chiba Institute of Technology, kenji.fujii@it-chiba.ac.jp*
[(3)] *Senior Staff, JFE Civil Engineering and Construction Corp., irie-chizuru@jfe-civil.com*
[(4)] *Senior Staff, JFE Civil Engineering and Construction Corp., tobari-ryota@jfe-civil.com*
[(5)] *Deputy General Manager, JFE Civil Engineering and Construction Corp., m-yoshinaga@jfe-civil.com*
[(6)] *General Manager, Dr. Eng., JFE Civil Engineering and Construction Corp., miyagawa@jfe-civil.com*

Abstract

The use of low-yield-strength steel damper columns in mid- and high-rise reinforced concrete (RC) buildings is widely recognized as an effective solution for reduction of the seismic response. However, in some cases, RC frames may be designed as “traditional” moment-resisting frames, which satisfy the current seismic design code of Japan without providing the effect of a damper column. Hence, steel damper columns installed in those frames are considered only as supplemental members. For the rational seismic design of such structures, it is preferable to consider the structural balance of RC frames and steel damper columns.

In recent years, seismic design has shifted from so-called force-based design to displacement-based design. In displacement-based seismic design, the properties of the structure are determined such that the response displacement for a given design earthquake does not exceed a predetermined limit. One motivation of installing dampers is reducing the displacement response, and the method of designing RC structures with dampers should thus be based on displacement. Studies have investigated displacement-based design procedures for RC frames with buckling-restrained braces. However, from the viewpoint of the authors, most of these studies focused on the method of determining the properties of buckling-restrained braces for predetermined RC frames. For better seismic design of such structures, the properties of RC frames should be adjusted considering the balancing of strength and stiffness between dampers and frames.

This paper presents a simple displacement-based seismic design method for RC frames with steel damper column. The proposed method is outlined as follows.

1. From the number of stories of the building considered, assume the equivalent height and equivalent mass of the equivalent single-degree-of-freedom (SDOF) model. Next, assume the yield displacement of RC frames and dampers and the ratio of the yield strength of RC frames and dampers.
2. Set the displacement limit of the equivalent SDOF model for the design seismic input.
3. Calculate the equivalent damping of the equivalent SDOF model at the displacement limit. Next, calculate the demand yield strength of the equivalent SDOF model using the equivalent linearization technique.
4. Determine the properties of the steel damper column for each story.
5. Determine the properties of the RC members, assuming that the locations of potential yield hinges are the ends of beams (except the beam ends connected to steel damper columns) and the bottom ends of the columns of the first story.

As a numerical example, the design of a 10-story RC frame building model is shown. The results of nonlinear time-history analysis show that the peak story drift of the building model is close to the predetermined design limit. The strength demand of the beam ends connected to the steel damper columns obtained in nonlinear time-history analysis and nonlinear static analysis are compared and discussed.

Keywords: Multi-story Reinforced Concrete Frame Structure, Steel Damper Column, Seismic Damping System, Displacement-controlled Seismic Design

1. Introduction

In the seismic design of new reinforced concrete (RC) buildings and the seismic retrofit of existing RC buildings, the use of energy-dissipating members (dampers) has recently become popular (e.g., [1]). However, in some cases, RC frames may be designed as "traditional" moment-resisting frames, which satisfy the current seismic design code of Japan without providing the effect of damper columns. Hence, steel damper columns installed in those frames are considered only as supplemental members. For the rational seismic design of such structures, it is preferable to consider the structural balance of RC frames and steel damper columns.

In recent years, seismic design has shifted from so-called force-based design to displacement-based design. In displacement-based seismic design, the properties of the structure are determined so that the response displacement for a given design earthquake does not exceed a predetermined limit (e.g., [2]). One motivation of installing dampers is reducing the displacement response, and the design method of RC structures with dampers should thus be based on displacement. Studies have addressed the displacement-based seismic retrofit design procedure for RC frames with buckling-restrained braces (e.g., [3]). However, from the viewpoint of the authors, most of those studies focused on the method of determining the properties of buckling-restrained braces for predetermined RC frames. For better seismic design of such structures, the properties of RC frames should be adjusted considering the balancing of strength and stiffness between dampers and frames.

This paper presents a simple displacement-based seismic design procedure for RC frames with steel damper columns. Then, as an example, a 10-story RC building with steel damper columns is designed and its seismic response is investigated through nonlinear static and dynamic (time history) analyses.

2. Outline of the Proposed Design Procedure

The building considered in this study is regular in both plan and elevation. Figure 1 shows the steel damper column considered in this study and the design yield mechanism of the RC frame. In the damper column shown in Figure 1(a), low-yield-strength steel is used for the shear panel, which absorbs the hysteresis energy [4]. In this study, the resistance of a damper column to out-of-plane loading is assumed negligible. All RC frames are designed according to the strong-column weak-beam concept except at the foundation level beam, and in the case of the steel damper column installed in an RC frame. In that case, at a connection joint of an RC beam with an installed steel damper column, the RC beam is designed to have strength sufficiently higher than the yield strength of the steel damper column considering strain hardening (Figure 1(b)).

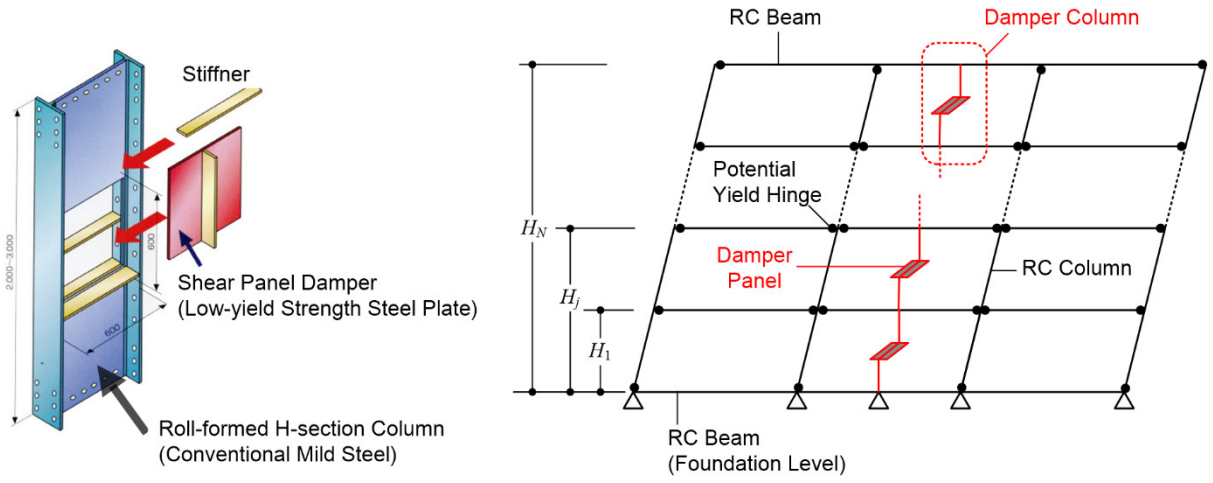

(a) Steel Damper Column (b) Design Yield Mechanism

Fig. 1 – Steel damper column and design yield mechanism of RC frames.

Figure 2 shows the flow of the design procedure. This study presents a simple displacement-based seismic design method for RC frames with steel damper columns. The concept of the design procedure is the same as that of the direct displacement-based seismic design presented in the literature [2]. The design ground motion is given in the form of an elastic response spectrum with 5% critical damping. The strength demand of the designed structure is determined adopting an equivalent single-degree-of-freedom (SDOF) model and equivalent linearization [5].

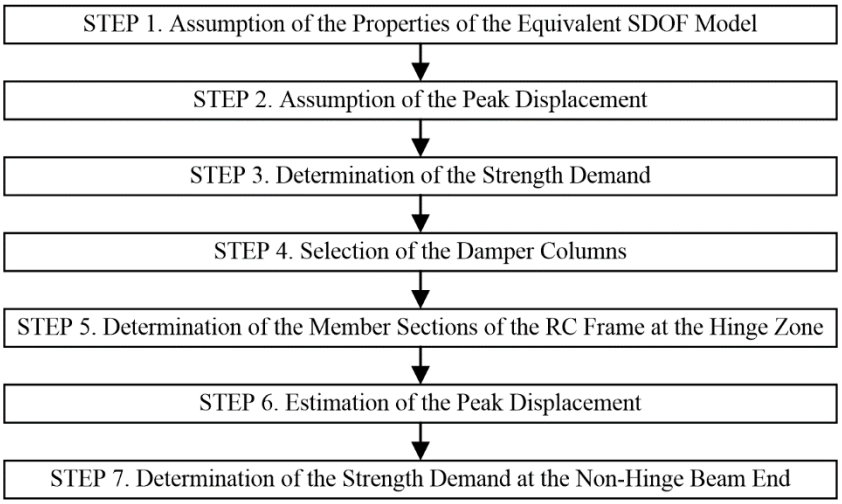

Fig. 2 – Flow of the design procedure.

The detail of the proposed procedure is as follows.

2.1 STEP 1: Assumption of the properties of the equivalent SDOF model

The equivalent mass M_1^* and equivalent height H_1^* are determined from the properties (i.e., the number of stories N, story height, area of each floor, and weight of the floor per unit area) of the building to be designed. To determine M_1^* and H_1^*, the first-mode vector $\Gamma_1\boldsymbol{\varphi}_1$ is approximated using an inverted triangle:

$$M_1^* = \Gamma_1\boldsymbol{\varphi}_1{}^{\mathrm{T}}\mathbf{M1} \approx \frac{\left(\mathbf{h}^{\mathrm{T}}\mathbf{M1}\right)^2}{\mathbf{h}^{\mathrm{T}}\mathbf{Mh}}, H_1^* = \frac{\Gamma_1\boldsymbol{\varphi}_1{}^{\mathrm{T}}\mathbf{Mh}}{M_1^*} \approx \frac{\mathbf{h}^{\mathrm{T}}\mathbf{Mh}}{\mathbf{h}^{\mathrm{T}}\mathbf{M1}}, \tag{1}$$

$$\mathbf{M} = \begin{bmatrix} m_1 & & 0 \\ & \ddots & \\ 0 & & m_N \end{bmatrix}, \mathbf{h} = \begin{Bmatrix} H_1 \\ \vdots \\ H_N \end{Bmatrix}, \mathbf{1} = \begin{Bmatrix} 1 \\ \vdots \\ 1 \end{Bmatrix}, \tag{2}$$

where $\mathbf{M}$ is the mass matrix, m_j (j = 1 to N) is the mass of the j-th floor, and H_j is the height of the j-th floor from the basement.

The ratio of the equivalent yield strength of dampers to RC frames, $r_Q = Q_{1yd}{}^* / Q_{1yf}{}^*$, and the equivalent yield drifts of dampers and RC frames, $R_{yd}{}^*$ and $R_{yf}{}^*$ respectively, are then assumed for the calculation of the equivalent damping at the assumed peak (target) displacement, h_{1eq}. For the simplicity, the ratio r_Q is assumed as the ratio of the number of damper columns in the considering direction to RC columns in each story.

2.2 STEP 2: Assumption of the peak displacement

The limit of the equivalent peak drift angle, $R_{limit}{}^*$, is determined considering the allowable damage level for the design ground motion. The assumed peak (target) displacement, $D_{1limit}{}^*$, is then assumed as the product of $R_{limit}{}^*$ and $H_1{}^*$.

2.3 STEP 3: Determination of the strength demand

The equivalent damping at $D_{1limit}{}^{*}$ is calculated as

$$h_{1eq} = \frac{h_{eqf} + r_Q h_{eqd}}{1 + r_Q}, \tag{3}$$

$$h_{eqf} = 0.20\left(1 - \sqrt{R_{yf}{}^{*} / R_{limit}{}^{*}}\right) + 0.05, h_{eqd} = 0.6 \times \frac{2}{\pi}\left(1 - R_{yd}{}^{*} / R_{limit}{}^{*}\right), \tag{4}$$

where h_{eqf} and h_{eqd} are respectively the equivalent damping ratios of RC frames and dampers. The equivalent (secant) period of the equivalent SDOF model T_{1eq} that satisfies the equation

$$S_D\left(T_{1eq}, h_{1eq}\right) = \frac{1.5}{1 + 10 h_{1eq}} S_D\left(T_{1eq}, 0.05\right) = D_{1limit}{}^{*} \tag{5}$$

is then found, where $S_D(T, 0.05)$ is the response displacement spectrum for the design ground motion. The yield strength demand of the equivalent SDOF model, $Q_{1y}{}^{*}$, is

$$Q_{1y}{}^{*} = M_1{}^{*} A_{1y}{}^{*} = M_1{}^{*}\left(2\pi / T_{1eq}\right)^2 D_{1limit}{}^{*}. \tag{6}$$

The equivalent yield strengths of the dampers and RC frame, $Q_{1yd}{}^{*}$ and $Q_{1yf}{}^{*}$ respectively, are

$$Q_{1yd}{}^{*} = \frac{r_Q}{1 + r_Q} Q_{1y}{}^{*}, Q_{1yf}{}^{*} = \frac{1}{1 + r_Q} Q_{1y}{}^{*}. \tag{7}$$

2.4 STEP 4: Selection of the damper column

The shear strength demand of the damper column for each story is determined from $Q_{1yd}{}^{*}$ obtained in STEP 3. The vertical distribution of the shear strength demand for the j-th story, Q_{ydn}, is assumed to be proportional to the story shear force distribution corresponding to the external force $\mathbf{p} = \mathbf{M}\left(\Gamma_1 \boldsymbol{\varphi}_1\right) A_{1y}{}^{*}$:

$$Q_{ydj} = \left(\sum_{k=j}^{N} m_k \Gamma_1 \varphi_{k1}\right) Q_{1yd}{}^{*} \Big/ M_1{}^{*} \approx \left(\sum_{k=j}^{N} m_k H_k \Big/ \sum_{k=1}^{N} m_k H_k\right) Q_{1yd}{}^{*}. \tag{8}$$

The proper damper column is then selected.

2.5 STEP 5: Determination of the member section of the RC frame

The design moment at the potential yield hinge section is determined from limit analysis such that the base shear of RC frames without damper columns is larger than the equivalent yield strength demand obtained in STEP 3, $Q_{1yf}{}^{*}$. To determine the section of RC beams, the size of the steel damper column is carefully considered such that it is not too weak and/or flexible compared with the damper column.

2.6 STEP 6: Estimation of the peak displacement

The lower bound (LB) model is constructed according to the selected damper column and determined RC member sections. The yield strength of all damper columns is assumed to be the initial yield strength of the damper panel, Q_{yDL}. Nonlinear properties of RC members are considered at potential hinge zones while simple linear behavior is considered at non-hinge member ends by assuming the stiffness of the cracked section (or a bilinear relationship is considered on the basis of the cracking of the member section).

Pushover analysis is then adopted and the peak response is predicted through equivalent linearization. The equivalent linearization technique has been detailed in the literature [6].

2.7 STEP 7: Determination of the strength demand at the non-hinge beam end

The upper bound (UB) model is constructed according to the selected damper column and determined RC member sections. The yield strength of all damper columns is assumed to be the UB of the yield strength after strain hardening due to appreciable cyclic loading of the damper panel, Q_{yDU}. The nonlinear properties of RC members are the same as those in the LB model.

Pushover analysis is then carried out and the peak response is predicted through equivalent linearization. The strength demand at the non-hinge beam end is the envelope of the results obtained from LB and UB models. The strength demand of the non-hinge zone at the RC column and shear strength demand of all RC members may be determined according to design guidelines [7].

3. Design Example

3.1 Building data

3.1.1 Example Building and Design Ground Motion

The example building has the 10-story RC moment-resisting frame shown in Figure 3. The span of beams is 7.5 m while the story height is 4.5 m for the first story and 3.2 m for the upper stories. The unit mass per floor is assumed to be 1.2 ton /m^2. Four damper columns are installed for each story in X- and Y-directions. The building structure is assumed pin supported.

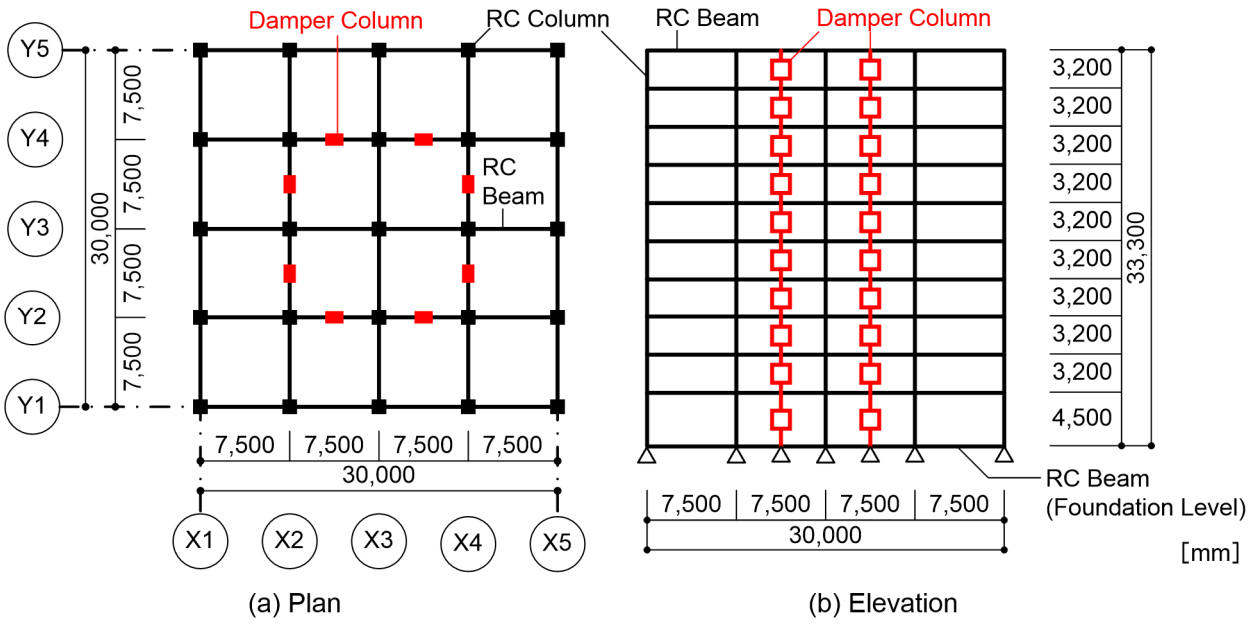

Fig. 3 – Plan and elevation of the model building.

The design ground motion is the spectrum taken from the Building Standard Law of Japan [8] with consideration of the type-2 soil condition. The pseudo acceleration spectrum with 5% critical damping is

$$ {}_pS_A(T,0.05) = \begin{cases} 4.8+45T \quad \mathrm{m/s^2} & T \le 0.16 \text{ s} \\ 12.0 & 0.16 \text{ s} \le T \le 0.864 \text{ s} \\ 12.0(0.864/T) & T > 0.864 \text{ s} \end{cases}, \tag{9} $$

where T is the natural period of the elastic SDOF model.

3.1.2 Design of an Example Building

Steps 1 through 5 of the design of the example building are carried out as follows.

In step 1, the equivalent mass and equivalent height of the equivalent SDOF model are calculated from the number of stories, story height, and floor areas using Eq. (1). The calculated equivalent mass M_1^* is 8734 ton while the equivalent height H_1^* is 18.34 m. The ratio of the equivalent yield strength of dampers to RC frames is assumed from the number of damper columns and RC columns in each story as $r_Q = 4/25 = 0.16$. The equivalent yield drift of RC frames R_{yf}^* is assumed as 1/150 while that of dampers R_{yd}^* is assumed as 1/500.

In step 2, the limit of the equivalent peak drift angle R_{limit}^* is assumed as 1/75. From this assumption, the assumed peak displacement is calculated as $D_{1limit}^* = 0.2445$ m.

In step 3, the equivalent damping ratio of RC frames and dampers are calculated using Eq. (4) as $h_{eqf} = 0.109$ and $h_{eqd} = 0.234$. The equivalent damping of the equivalent SDOF model is then calculated using Eq. (3) as $h_{1eq} = 0.126$. Next, the equivalent (secant) period is estimated using Eq. (5) as $T_{1eq} = 1.402$ s. Figure 4 shows the estimation of T_{1eq} and A_{1y}^* adopting the equivalent linearization technique. For $h_{1eq} = 0.126$, the reduced ${}_pS_A$–S_D relationship is drawn as the blue curve. Then from $S_D(T_{1eq}, 0.126) = D_{1limit}^* = 0.2445$ m, A_{1y}^* is easily obtained as the intersection of the reduced ${}_pS_A$–S_D curve and the vertical dotted line ($D_1^* = 0.2445$ m); i.e., 4.91 m/s^2. The equivalent period is obtained from the tangent of the dotted line as $T_{1eq} = 2\pi(0.245/4.91)^{0.5} = 1.402$ s.

Ratio of the yielding strength : $r_Q = 0.16$
Equivalent yield drift of RC frames: $R_{yf}^* = 1/150$
Equivalent yield drift of dampers : $R_{yd}^* = 1/500$
Limit of equivalent peak drift : $R_{limit}^* = 1/75$
Equivalent damping of equivalent SDOF model:

$$h_{1eq} = \frac{0.109 + 0.16 \cdot 0.234}{1 + 0.16} = 0.126$$

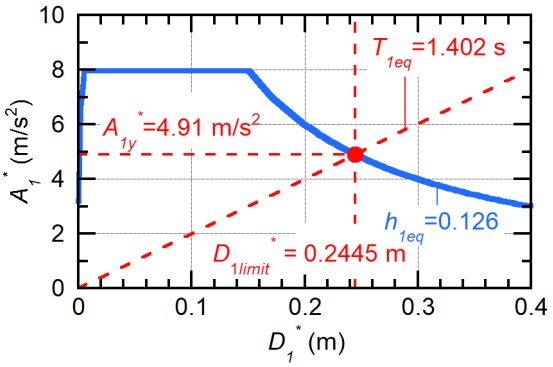

Fig. 4 – Estimation of T_{1eq} and A_{1y}^*.

From Eq. (6), the yield strength demand of the equivalent SDOF model is determined as $Q_{1y}^* = 8734$ ton × 4.91 m/s^2 = 42.88 MN. Therefore, from Eq. (7), the equivalent yield strengths of dampers and RC frames are respectively determined as $Q_{1yd}^* = 5.914$ MN and $Q_{1yf}^* = 36.97$ MN.

In step 4, the shear strength demand of damper columns of each story is determined for $Q_{yd}^* = 5.914$ MN, considering the vertical distribution of the shear strength demand proportional to the story shear strength demand corresponding to $\mathbf{p} = \mathbf{M}(\Gamma_1 \boldsymbol{\varphi}_1) A_{1y}^*$. Table 1 lists the selected damper columns. The damper columns are chosen from a catalog provided by JFE Civil Corporation Engineering Co. Ltd. [9] such that the sum of the LB strength Q_{yDL} of damper columns is larger than the shear strength demand for each story. The initial normal yield stress of the steel used for damper panels is assumed as 205 N/mm^2 while the nominal yield stress after appreciable cyclic loading is assumed as 300 N/mm^2.

Table 1 – Selected damper columns

Story	Yield Strength		Panel Thickness	Panel Sectional Area	Column
	Q_{yDL} (kN)	Q_{yDU} (kN)	t_p (mm)	A_{SDd} (mm^2)	(mm × mm × mm × mm)
10	438	641	6	3,700	H - 600 × 200 ×12 × 25
9	626	916	9	5,290	H - 600 × 250 ×16 × 32
8	755	1,105	9	6,380	H - 700 × 300 ×16 × 28
7	968	1,417	9	8,180	H - 900 × 300 ×16 × 28
5 to 6	1,251	1,831	9	10,580	H - 600 × 250 ×16 × 32 × 2
1 to 4	1,511	2,211	9	12,760	H - 700 × 300 ×16 × 28 × 2

In step 5, the design moment at the potential hinge of RC beams, M_y, is determined from (a) the moment obtained in the limit analysis of the RC frame without a damper column based on the principal of virtual work and (b) the moment calculated from the equilibrium condition at the connection of RC beams with steel damper columns, assuming the shear force of the damper column is equal to Q_{yDL} and an anti-symmetrical distribution of the bending moment, for consideration of the strength balance of RC beams and steel damper columns at non-hinge beam ends. In this study, M_y, is taken as the maximum of the values obtained in (a) and (b).

Figure 5 shows the determination of the design moment of the beam at the potential hinge while Table 2 lists sections at potential hinges. Note that the cross sections for all RC columns are 900 mm × 900 mm, which is the same as the cross section at the bottom of the first story. The cross sections of the RC beams at the foundation level are 800 mm × 1900 mm. The yield strength of the longitudinal reinforcement is assumed as $\sigma_y = 1.1 \times 390 = 429$ N/mm^2. The assumed compressive strength of concrete is 33 N/mm^2 for the first and second stories, 30 N/mm^2 for the third to fifth stories, and 27 N/mm^2 above the sixth story.

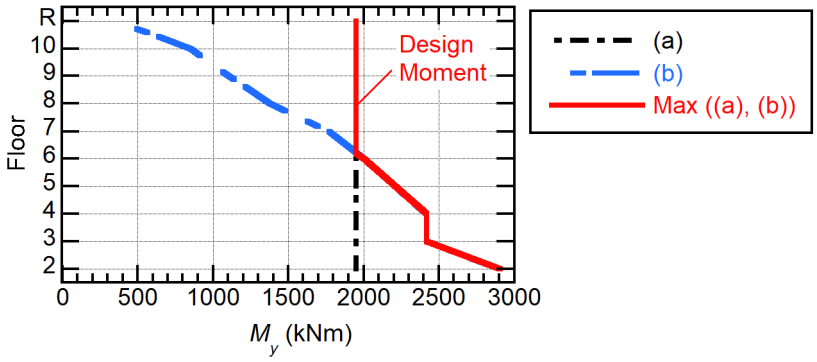

Fig. 5 – Determination of the design beam strength.

Table 2 – Sections at potential hinges

Member	Location	Width b (mm)	Depth D (mm)	Longitudinal reinforcement
Beam	7th to Roof floor	500	900	10 – D29 (Top and bottom)
	6th floor	550	900	8 – D32 (Top and bottom)
	5th floor	550	900	9 – D32 (Top and bottom)
	3rd to 4^{h} floor	600	900	8 – D35 (Top and bottom)
	2nd floor	800	900	9 – D38 (Top and bottom)
Column	1st Story (Bottom)	900	900	24 – D29

3.1.3 Modeling of the Structure

The building is modelled as a plane frame model. All frames are connected through a rigid slab. Figure 6 shows a model of the frame. A rigid zone is considered at each member end. For the RC beams connected to the RC columns, the length of the rigid zone is assumed as half the depth of the intersected column minus one-fourth the depth of the considered beam, while the length of the rigid zone of each RC column is assumed as half the depth of the intersected beam minus one-fourth the depth of the considered column. Additionally, for beams connected to a steel damper column, the length of the rigid zone is assumed as half the depth of the intersected damper column while the length of the rigid zone of each steel damper column is assumed as half the depth of the intersected beam (i.e., 0.45 m). All RC members are modelled as a one-component model with a nonlinear flexural spring at each end while steel damper columns are modelled as an elastic column with a nonlinear shear spring in the middle.

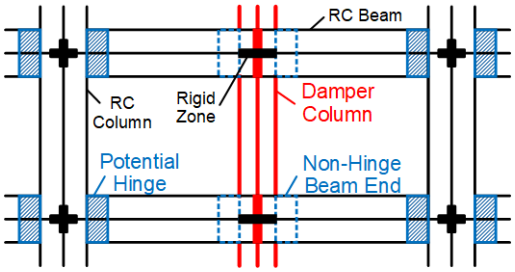

Fig. 6 – Modeling of the frame.

Figure 7 shows envelopes of the force–deformation relationship of members. The envelopes are assumed to be symmetric in positive and negative loading directions. In this figure, M_c and M_y are respectively the crack and yield moments of RC members while θ_c and θ_y are respectively the crack and yield rotational angles of RC members. For the calculation of M_c and M_y of each RC column, only the axial force attributed to the vertical load is considered. In Figure 7(a), the secant stiffness degradation ratio (α_y) of the flexural spring at the yield point is calculated according to Sugano's equation following Koreishi [10]. Note that at a non-hinge member end (i.e., a beam end connected to a damper column, or a column end except that at the bottom of the first story), the bilinear envelope shown in Figure 7(b) is assumed except a beam at the foundation level; i.e., the tangent stiffness degradation ratio after cracking (α_1) is assumed as 0.2 for the non-hinge ends of RC columns while the same value as for the opposite side end is used at a non-hinge end of an RC beam. The flexural behavior of a beam at the foundation level is assumed linear elastic. The shear behavior of all RC members is assumed linear elastic. In nonlinear static analysis, the bilinear envelope shown in Figure 7(c) is assumed for the damper panel. In Figure 7(c), γ_{yDL} and γ_{yDU} are respectively the yield shear angle of the damper panel for LB and UB models. The axial behavior of all vertical members is assumed to be linearly elastic.

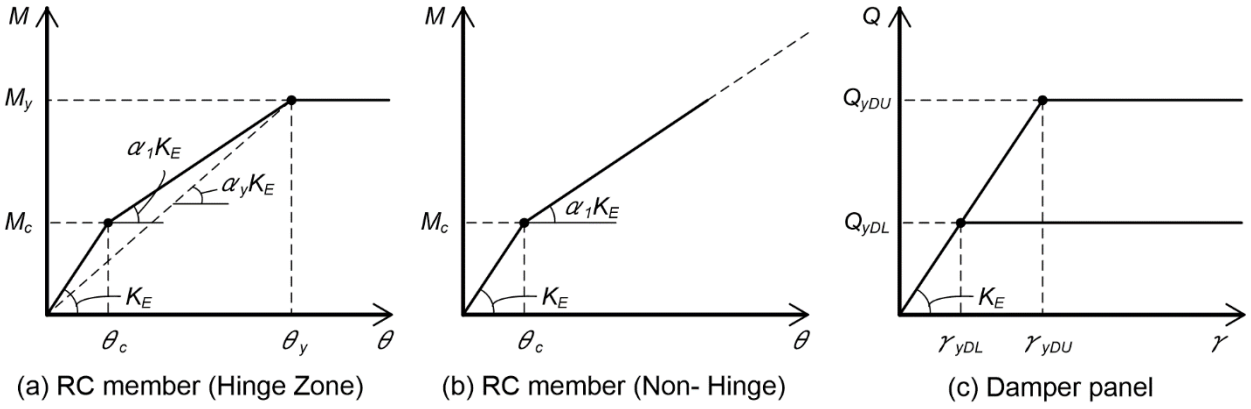

Fig. 7 – Envelope of the force–deformation relationship.

In nonlinear time history analysis, the Muto hysteresis model [11] with one modification is used to model the flexural spring in RC members, as in a previous study [6], while the hysteresis model proposed by Ono and Kaneko [12] is used to model the shear behavior of the damper columns with consideration of the strain–hardening behavior. Note that the initial yield strength of the damper panel is assumed as Q_{yDL} while the UB yield strength is assumed as Q_{yDU}, as in a previous study [13].

The damping matrix is assumed to be proportional to the instant stiffness matrix without a damper column. The damping ratio of the elastic first mode of the model without a damper column is assumed as 0.05.

3.2 Ground Motion

Three artificial ground motions are generated. The target elastic spectrum with 5% critical damping is the same as that of the design ground motion (i.e., Eq. (9)). Figure 8 shows the pseudo acceleration spectrum and time history of the generated ground motions.

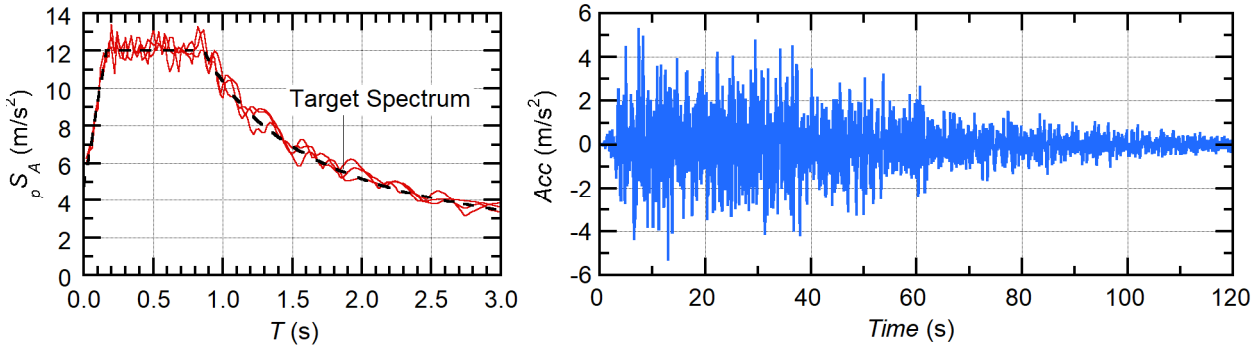

(a) Psuedo Acceleration Spectrum (b) Acceleration

Fig. 8 – Ground motions used in the nonlinear time history analysis.

4. Analysis Results

This section evaluates the seismic response of the example building designed through steps 1 to 5 adopting nonlinear time-history analysis. The strength demand at the non-hinge beam end (i.e., the beam end connected to the damper column) predicted by nonlinear static analysis using the UB model is then compared with the results of time-history analysis. These results correspond to steps 6 and 7 in the presented design procedure.

4.1 Nonlinear static analysis

Figure 9 shows the relationship of the equivalent acceleration A_1^* versus equivalent displacement D_1^* of the LB and UB models obtained from displacement-based mode-adaptive pushover analysis (DB-MAP analysis) [14]. The equivalent acceleration and displacement at step n, ${}_nA_1^*$ and ${}_nD_1^*$ respectively, are calculated from the pushover analysis results as

$$ {}_nA_1^* = \frac{{}_n\Gamma_{1\,\mathbf{n}}\boldsymbol{\varphi}_1^{\mathrm{T}}\,{}_n\mathbf{f_R}}{{}_nM_1^*} = \frac{{}_\mathbf{n}\mathbf{d}^{\mathrm{T}}\,{}_n\mathbf{f_R}}{{}_\mathbf{n}\mathbf{d}^{\mathrm{T}}\mathbf{M1}},\ {}_nD_1^* = \frac{{}_n\Gamma_{1\,\mathbf{n}}\boldsymbol{\varphi}_1^{\mathrm{T}}\mathbf{M}_\mathbf{n}\mathbf{d}}{{}_nM_1^*} = \frac{{}_\mathbf{n}\mathbf{d}^{\mathrm{T}}\mathbf{M}_\mathbf{n}\mathbf{d}}{{}_\mathbf{n}\mathbf{d}^{\mathrm{T}}\mathbf{M1}}, \tag{10} $$

$$ {}_\mathbf{n}\mathbf{d} = \left\{ {}_ny_1 \quad {}_ny_2 \quad \cdots \quad {}_ny_N \right\}^{\mathrm{T}},\ {}_\mathbf{n}\mathbf{f_R} = \left\{ {}_nf_{R1} \quad {}_nf_{R2} \quad \cdots \quad {}_nf_{RN} \right\}^{\mathrm{T}}, \tag{11} $$

where ${}_\mathbf{n}\mathbf{d}$ and ${}_\mathbf{n}\mathbf{f_R}$ are respectively the displacement and restoring-force vector at step n. Note that in equation (10), the first-mode vector at step n of DB-MAP analysis, ${}_n\Gamma_{1\,\mathbf{n}}\boldsymbol{\varphi}_1$, is assumed to be proportional to the displacement vector. The contributions of RC frames and damper columns to the equivalent acceleration, ${}_nA_{1f}^*$ and ${}_nA_{1d}^*$ respectively, are calculated as

$$ {}_nA_{1f}{}^{*} = \frac{{}_n\Gamma_1\,{}_n\boldsymbol{\varphi}_1{}^{\mathrm{T}}\,{}_n\mathbf{f}_{\mathbf{Rf}}}{{}_nM_1{}^{*}} = \frac{{}_n\mathbf{d}^{\mathrm{T}}\,{}_n\mathbf{f}_{\mathbf{Rf}}}{{}_n\mathbf{d}^{\mathrm{T}}\mathbf{M1}},\ {}_nA_{1d}{}^{*} = \frac{{}_n\Gamma_1\,{}_n\boldsymbol{\varphi}_1{}^{\mathrm{T}}\,{}_n\mathbf{f}_{\mathbf{Rd}}}{{}_nM_1{}^{*}} = \frac{{}_n\mathbf{d}^{\mathrm{T}}\,{}_n\mathbf{f}_{\mathbf{Rd}}}{{}_n\mathbf{d}^{\mathrm{T}}\mathbf{M1}}, \tag{12} $$

$$ {}_n\mathbf{f}_{\mathbf{Rf}} = \left\{ {}_nf_{Rf1} \quad {}_nf_{Rf2} \quad \cdots \quad {}_nf_{RfN} \right\}^{\mathrm{T}},\ {}_n\mathbf{f}_{\mathbf{Rd}} = \left\{ {}_nf_{Rd1} \quad {}_nf_{Rd2} \quad \cdots \quad {}_nf_{RdN} \right\}^{\mathrm{T}}, \tag{13} $$

where ${}_n\mathbf{f}_{\mathbf{Rf}}$ and ${}_n\mathbf{f}_{\mathbf{Rd}}$ are respectively the restoring force vectors of RC frames and steel dampers at step *n*. Note that the restoring-force vector ${}_n\mathbf{f}_{\mathbf{R}}$ is equal to the sum of ${}_n\mathbf{f}_{\mathbf{Rf}}$ and ${}_n\mathbf{f}_{\mathbf{Rd}}$, which are respectively calculated from the shear forces of RC columns and steel damper columns. The dotted horizontal lines in Figure 9(a) indicate $A_{1y}{}^{*} = Q_{1y}{}^{*}/M_1{}^{*}$, $A_{1yf}{}^{*} = Q_{1yf}{}^{*}/M_1{}^{*}$, and $A_{1yd}{}^{*} = Q_{1yd}{}^{*}/M_1{}^{*}$ estimated in step 3 while the dotted vertical lines indicate the assumed peak displacement $D_{1limit}{}^{*}$. The peak responses predicted adopting the equivalent linearization technique are also shown for both the LB and UB models. The results of pushover analysis presented in Figure 9(a) show that the designed building structure satisfies the equivalent strength demand determined in step 3.

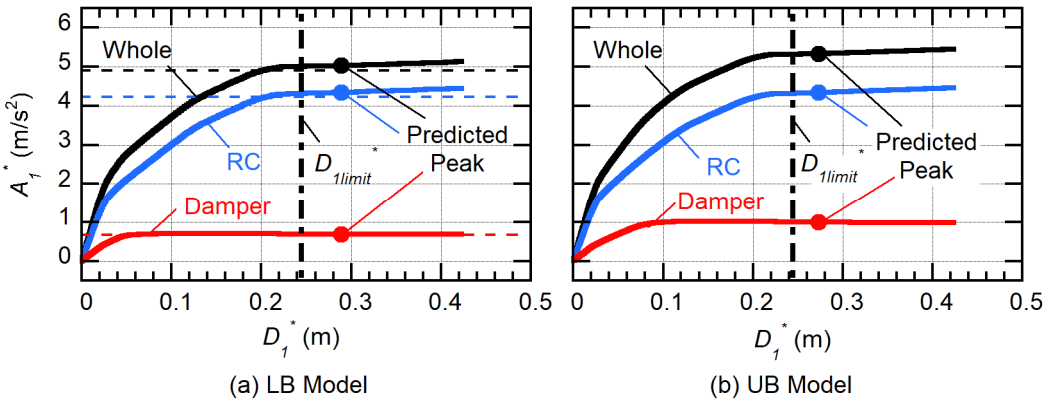

Fig. 9 – Properties of equivalent SDOF models.

In Figure 9, the peak responses predicted using LB and UB models exceed the assumed peak displacement $D_{1limit}{}^{*}$. One reason is that, in the pushover analysis, the vertical distribution of horizontal displacement differs from an inverted triangle; i.e., the story drift for upper stories is smaller than that for lower stories, and RC beams of the upper stories do not yield. Another reason is that adoption of the equivalent linearization technique applied here results in predictions that are too conservative as discussed later.

4.2 Comparisons of the peak response obtained from nonlinear time-history analysis

Figure 10 compares the peak response obtained from the nonlinear static analysis and the nonlinear time-history analysis results. As shown in Figure 10 (a), the peak story drift obtained from nonlinear time-history analysis is close to the limit of the equivalent peak drift angle ($R = R_{limit}{}^{*} = 1/75$) for the lower stories and smaller for the upper stories, although the peak story drifts obtained from static analysis with the LB and UB models are larger than 1/75. The normalized shear force of damper columns ($Q_{D\max}/Q_{yDL}$) obtained from the nonlinear time-history analysis is close to the static analysis results obtained using the UB model, as shown in Figure 10(b). The maximum moment at the non-hinge beam end obtained from the static analysis results of the UB model is slightly smaller than the nonlinear time history analysis results, as shown in Figure 10(c).

For the example building considered in this study, the peak drift predicted by nonlinear static analysis using the LB model is too conservative. The estimation of the peak displacement from the pushover analysis of the LB model corresponds to STEP 6 of the proposed design procedure, and the accuracy of the evaluated peak drift may therefore be acceptable for preliminary design purposes. However, improvements in the prediction of the peak response may be needed. According to the determination of the strength demand at the non-hinge beam end in STEP 7, nonlinear static analysis using the UB model may be applicable for preliminary design purposes.

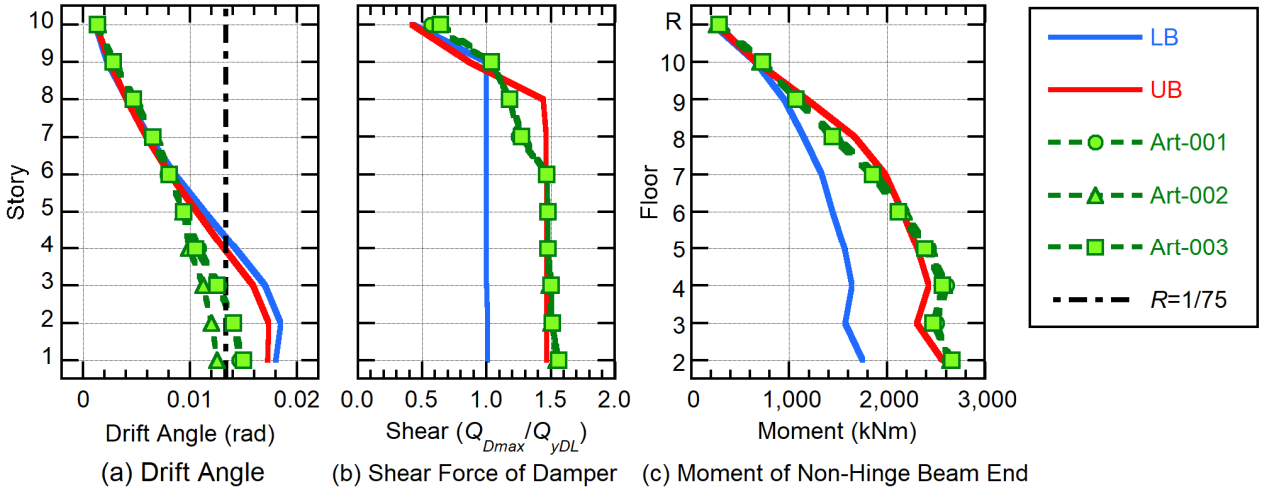

Fig. 10 – Comparisons of peak responses.

5. Conclusions

A simple displacement-based seismic design procedure for RC frames with steel damper columns was presented. As an example, a 10-story RC building with steel damper columns was designed and its seismic response was investigated in nonlinear static and time-history analysis. The main contributions and results of the paper are as follows.

(1) The presented simplified displacement-based seismic design procedure successively controls the peak drift of an example 10-story RC building. The largest peak drift obtained from the results of time-history analysis is close to the predetermined drift limit. However, the peak response predicted in nonlinear static analysis using the LB model is too conservative.

(2) The strength demand at the non-hinge beam end can be evaluated from pushover analysis using the UB model. However, since the evaluated result is slightly smaller than the nonlinear time-history analysis results, margin of safety is needed for the design purpose.

Only one example was presented in this paper. Further investigations for different numbers of stories and a vertical distribution of damper columns are needed to validate the design procedure. It is also important to improve the technique of predicting the nonlinear peak displacement of the equivalent SDOF model representing RC structures with hysteresis dampers.

Acknowledgment

We thank Glenn Pennycook, MSc, from Edanz Group (www.edanzediting.com/ac) for editing a draft of this manuscript.

References

[1] Izumi N, Chiba O, Takahashi K, and Iizuka S (2004): Earthquake resistant performance of reinforced concrete frame with energy dissipation devices. *13th World Conference on Earthquake Engineering*, 1 – 6 August, Vancouver, Canada.

[2] Priestley MJN, Kowalsky MJ (2000): Direct displacement-based seismic design of concrete buildings. *Bulletin of the New Zealand Society for Earthquake Engineering*, **33** (4), 421-444.

[3] Mazza F, Vulcano A (2014): Displacement-based design procedure of damped braces for the seismic retrofitting of r.c. framed buildings. *Bulletin of Earthquake Engineering*, **13**(7), 2121-2143.

[4] Katayama T, Ito S, Kamura H, Ueki T, Okamoto, H (2000): Experimental study on hysteretic damper with low yield strength steel under dynamic loading. *12th World Conference on Earthquake Engineering*, 30 January – 4 February, Auckland, New Zealand.

[5] Otani S (2000): New seismic design provision in Japan. *Proceedings of the second US–Japan workshop on performance-based earthquake engineering methodology for reinforced concrete structures*, PEER Report 2000/10, 3–14.

[6] Fujii K, Miyagawa K (2018): Nonlinear seismic response of a seven-storey steel reinforced concrete condominium retrofitted with low-yield-strength-steel damper columns. *16th European Conference on Earthquake Engineering*, 18 –21 June, Thessaloniki, Greece.

[7] AIJ (2019): *AIJ seismic performance evaluation guideline for reinforced concrete buildings based on the capacity spectrum method*, Architectural Institute of Japan.

[8] BCJ (2016): *The Building standard law of Japan on CD-ROM*, The Building Center of Japan.

[9] JFE Civil Engineering & Construction Corp. (2019), JFE no Seishin-mabashira, JFE no Seishin-panel (*Vibration control column and panel product by JFE*). Available online, https://www.jfe-civil.com/pdf/catalog/vibration_control_column.pdf (last accessed on 25th January 2020, in Japanese)

[10] Sugano S Koreishi, I (1974): An empirical evaluation of inelastic behaviour of structural elements in reinforced concrete frames subjected to lateral forces. *5th World Conference on Earthquake Engineering*, 25-29, June, Rome, Italy.

[11] Muto K, Hisada T, Tsugawa T, Bessho S (1974): Earthquake resistant design of a 20 story reinforced concrete buildings, *5th World Conference on Earthquake Engineering*, 25-29, June, Rome, Italy.

[12] Ono Y, Kaneko H (2001): Constitutive rule of the steel damper and source code for the analysis programs, *Passive control symposium*, Structural Engineering Research Center, Tokyo Institute of Technology, 14–15 December, Yokohama, Japan. (in Japanese)

[13] Fujii K, Sugiyama H, Miyagawa K (2019): Predicting the peak seismic response of a retrofitted nine-storey steel reinforced concrete building with steel damper columns. *WIT Transactions on The Built Environment*, **185**, 75-85.

[14] Fujii K (2014): Prediction of the largest peak nonlinear seismic response of asymmetric buildings under bidirectional excitation using pushover analyses, *Bulletin of Earthquake Engineering*, **12**, 909-938.

